Field of view effects on local slope measurements in confocal laser scanning microscopy for surface metrology

S. Gao, A. Felgner, T. Dziomba
Physikalisch-Technische Bundesanstalt, Bundesallee 100, Braunschweig, Germany

ABSTRACT

Surface-dependent field-of-view (FOV) inhomogeneity in confocal laser scanning microscopy (CLSM) has been demonstrated but remains insufficiently quantified, particularly for surfaces with complex, multi-scale geometries. This limitation affects the traceability and comparability of optical surface topography measurements. In this work, we show that FOV-induced measurement deviations are fundamentally surface-dependent and cannot be explained by local slope alone. Using deterministic and stochastic surfaces with controlled slope distributions and spatial frequency content, we demonstrate that smooth geometries exhibit negligible FOV effects, whereas complex high-frequency surfaces exhibit pronounced position-dependent distortions. To interpret this phenomenon, a surface-complexity-driven framework is introduced, linking the angular transfer characteristics of the instrument to the surface slope distribution via a complexity parameter ξ. By relating ξ to gradient magnitude distribution descriptors (e.g., *Sdq95*) and spatial frequency characteristics (e.g., *Sal*), the framework provides a physically grounded interpretation of FOV-dependent measurement limits. The results indicate that, for complex surfaces, CLSM measurements become increasingly instrument-limited rather than surface-limited, due to position-dependent loss of high-angle information. The observed FOV effects are consistent with scanning-induced angular limitations, including pupil shift and/or clipping, and off-axis aberrations. This work establishes a foundation for task-specific, traceable optical metrology of complex surfaces.

Keywords: surface texture metrology, confocal laser scanning microscopy, field of view homogeneity, slope measurement capability

1. INTRODUCTION

Three-dimensional (3D) optical microscopy has become an essential tool in modern surface metrology due to its capability for rapid, non-contact, and non-destructive measurement of surface topography [1-3]. Among the available techniques, confocal laser scanning microscopy (CLSM) is widely used for areal surface characterization, offering high lateral resolution and flexibility across different surface types [4-5]. However, despite its widespread adoption, achieving traceability, comparability, and reliability of optical measurements remains a major metrological challenge [6-7].

The core difficulty arises from the complex interaction between illumination light and surface features. Measurement results are not solely determined by the instrument, but are also strongly influenced by intrinsic surface characteristics, such as spatial frequency content, local slope distribution, and structural complexity. In particular, surfaces with steep slopes often lead to systematic deviations in measured topography parameters.

Previous studies have indicated that field-of-view (FOV) inhomogeneity is a critical factor affecting measurement fidelity in CLSM [8]. Measurements performed at different positions within the FOV may yield inconsistent results, even when observing the same surface. This effect becomes especially pronounced for surfaces with high local slopes and complex geometries. However, a systematic and quantitative understanding of how FOV position influences slope detection limits and measurement deviations remains limited.

Despite extensive studies on instrument transfer behavior and surface complexity [9-10], a quantitative framework linking angular acceptance, surface structure, and position-dependent measurement response is still missing.

In this work, we investigate the influence of FOV position on topography measurements in CLSM using both deterministic and stochastic surface geometries. By comparing spherical, milled, and rough surfaces with different spatial frequency content and slope distributions, we establish a surface-dependent framework for describing FOV-induced measurement limitations. Ultimately, this work contributes to the development of traceable, surface-dependent optical metrology frameworks for complex surfaces.

*sai.gao@ptb.de; phone +49 531 592 5167; www.ptb.de

2. EXPERIMENTAL CHARACTERIZATION OF SURFACE-DEPENDENT FOV EFFECTS IN CLSM MEASUREMENTS

All experimental investigations of surface-dependent FOV effects in this study were performed using a commercial CLSM equipped with a 50× objective (NA = 0.95). The corresponding FOV is 258 µm × 258 µm, with an image resolution of 1024 × 1024 pixels. Prior to measurement, the system was calibrated in accordance with ISO 25178-700 [11] using traceable geometric standards.

Reference AFM measurements were performed at five locations within the objective's FOV on an ARS f2 surface (SiMetrics) [12], a lapped silicon surface characterized by high spatial-frequency content and significant local slopes, representing a challenging test case for optical topography measurements. A comparison of the areal height parameters *Sa* and *Sq* between AFM and CLSM reveals clear FOV-dependent variations, indicating measurement inhomogeneity across the FOV [8].

Considering the point-by-point scanning principle of CLSM [13], in which scan mirrors laterally deflect the laser beam across the sample, it is hypothesized that the scanning angle influences the effective angular acceptance of the objective. With increasing scanning angle, i.e., towards the edges of the FOV, the beam enters the objective pupil under increasingly off-axis conditions. This results in pupil shift and partial pupil clipping, accompanied by increased off-axis aberrations, which together reduce the effective collection of high-angle scattered or reflected light [14].

As a consequence, the maximum measurable surface slope is expected to decrease towards the FOV boundaries. Surface features with large local slopes, such as those present on the ARS f2 surface, which can be measured with low uncertainty near the FOV center, may therefore be incompletely or inaccurately captured near the edges of the FOV. This leads to systematic measurement artefacts, including overshooting, and consequently to overestimated height parameters.

To quantitatively assess the slope-dependent measurement capability, a set of representative samples was investigated, comprising two deterministic geometries and two types of rough surfaces: (1) a spherical artefact (continuous slope variation); (2) a 4 µm pitch grating (90 nm height, high spatial-frequency content); (3) real milled technical surfaces (narrower slope distribution, larger autocorrelation length); and (4) the ARS f2 surface (broader slope distribution, shorter autocorrelation length).

2.1 Deterministic Geometries

Figure 1 shows measured topography images of a 120 µm diameter ruby sphere acquired at different positions within the FOV, together with the corresponding horizontal profiles taken through the sphere center. After alignment, the profiles exhibit excellent agreement, indicating that the maximum measurable slope, or equivalently, the effective numerical aperture, remains uniform across the FOV. This confirms the absence of significant position-dependent measurement deviations for this geometry.

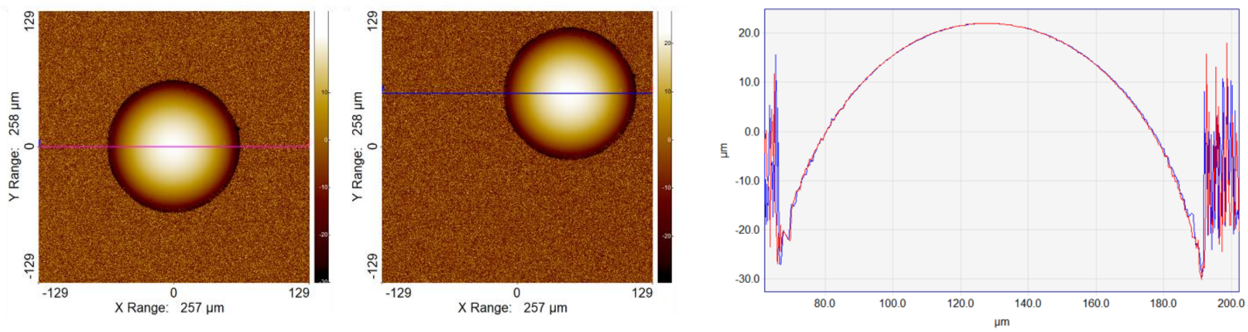

(a) Measured topography images. (b) The horizontal profiles through the sphere center.

Figure 1. Measured topography images of a 120 µm diameter ruby sphere at different FOV positions, obtained using a CLSM with a 50× objective (NA 0.95), with corresponding profiles. No significant position-dependent measurement deviation across the FOV.

Figure 2 shows the measurement result of a 4 µm pitch grating with a height of 90 nm, measured at the spatial resolution limit of the 50× objective used in the CLSM. Prior reference measurements confirmed that the grating is homogenous.

Figure 2. (b) presents three cross-sectional profiles taken at different vertical positions within the FOV. An evident increase in overshooting is observed toward the edges of the FOV, indicating significant position-dependent measurement effects across the field.

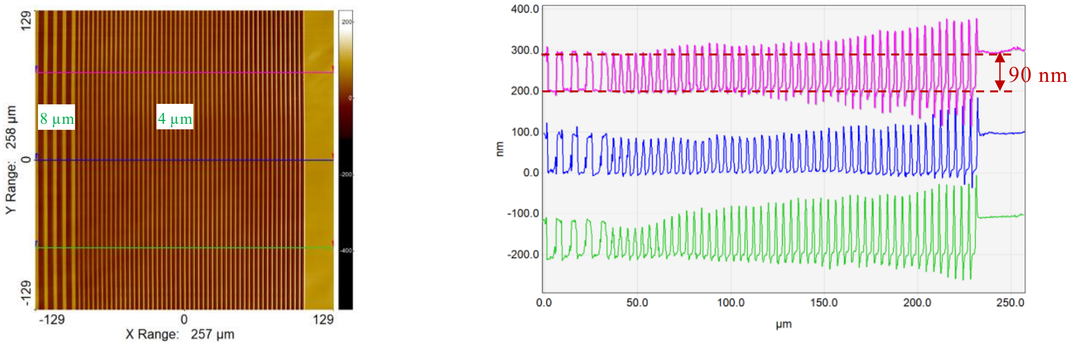

(a) Measured topography image of the grating. (b) The horizontal profiles at different positions within the FOV.

Figure 2. Measured topography images of a 4 µm pitch grating, obtained using a CLSM with a 50× objective (NA 0.95), with corresponding profiles. Significant position-dependent measurement deviation across the FOV.

The results suggest that surfaces with low spatial frequency content and gradual slope variation can be measured robustly by CLSM, showing negligible sensitivity to FOV inhomogeneity. In contrast, measurements of a grating structure with a pitch of 4 µm exhibit distinctly different behavior. Although the geometry is deterministic, the presence of higher spatial frequency components leads to observable variations in the measured signal across the FOV. This indicates that even periodic structures can exhibit sensitivity to FOV effects when their spatial frequency content approaches the instrument's resolution or angular detection limits.

2.2 Rough surfaces

To investigate realistic measurement scenarios, rough surfaces with varying complexity were analyzed, including several milled surfaces and the ARS f2 surface. The measurement strategy consisted of selecting a sub-area (e.g., 30 µm × 30 µm) and repositioning this identical region to different locations within the FOV, enabling a direct comparison of the measurement results obtained at different FOV positions. Figure 3 illustrates this approach, in which the selected region (no. 1) is shifted along a 45° direction across the FOV.

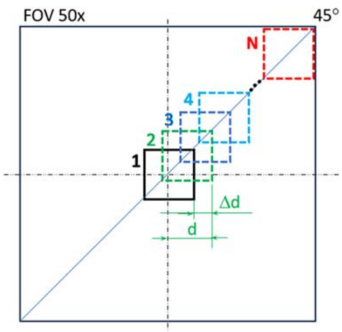

Figure 3. Schematic of the measurement steps to investigate the inhomogeneity of the FOV of a CLSM, Δd is the in-plane shift of each step and d is the distance from the right border of the shifted test region to the center of the FOV.

Figure 4 presents the evaluated *Sa* and *Sq* values of the test region for both the ARS f2 and a milled surface at different FOV positions, together with the corresponding local slope distributions measured at the center and edge of the FOV.

As shown in Figure 4(a), the *Sq* and *Sa* values of the ARS f2 test region remain stable within a central measurement range of 90 µm (d = 45 µm), but change significantly outside this region. The *Sq* values at the first and last measurement positions are 79.8 nm and 176 nm, respectively, corresponding to a relative increase of 121%. In contrast, Figure 4(c) shows that for the milled surface, the *Sq* (and *Sa*) values vary only slightly across the entire FOV, with *Sq* increasing by just 1.6 nm.

Figures 4(b) and 4(d) present the corresponding local slope distributions of a 30 µm × 30 µm region for both samples, measured at the center and edge positions. For the milled surface, the slope distributions remain largely unchanged. In contrast, for the more complex ARS f2 surface, the slope distribution at the edge position becomes significantly broader than at the center, indicating the increasing influence of measurement artefacts such as overshooting.

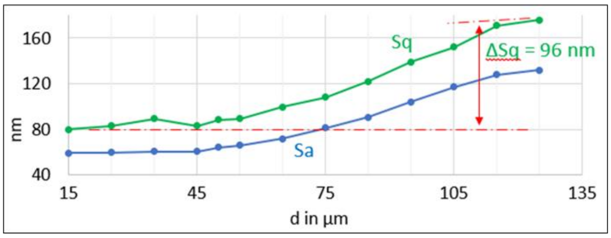

(a) *Sa* and *Sq* values of the central 30 µm x 30 µm region of the ARS f2 surface measured at different positions along 45° direction within the FOV

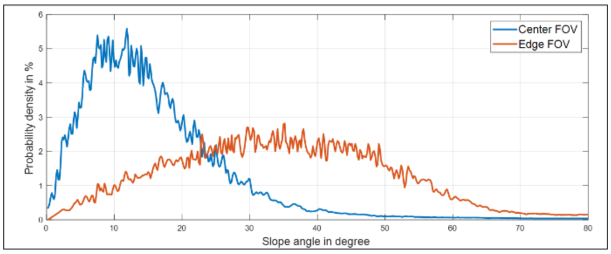

(b) Local slope distributions of the 30 µm x 30 µm region of the ARS f2 surface measured at center and edge positions along 45° direction within the FOV

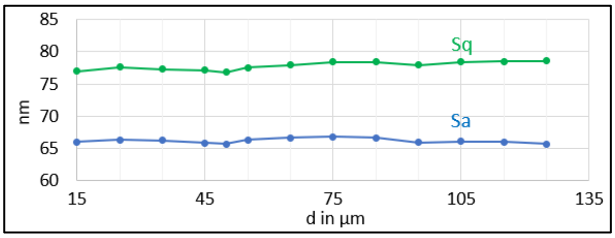

(c) *Sa* and *Sq* values of the central 30 µm x 30 µm region of the milled surface measured at different positions along 45° direction within the FOV

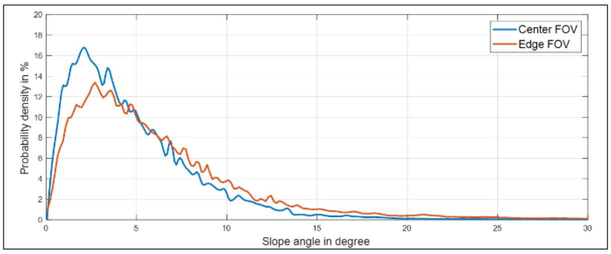

(d) Local slope distributions of the 30 µm x 30 µm region of the milled surface measured at center and edge positions along 45° direction within the FOV

Figure 4. Surface-dependent field-of-view effects on measured surface textures in CLSM measurements.

These results clearly demonstrate that FOV-induced deviations are not governed by slope alone, but are strongly influenced by the combined effect of slope distribution and surface structure. This observation highlights that surfaces with similar slope ranges may exhibit fundamentally different measurement behavior depending on their structural complexity, motivating the introduction of the surface complexity descriptor ξ in the following section.

3. PHYSICS-BASED SEMI-ANALYTICAL MODEL OF INSTRUMENT-INDUCED FOV DISTORTIONS

3.1 Surface complexity descriptor

To account for the influence of multi-scale geometry and surface-dependent interactions, a surface complexity descriptor ξ is introduced:

$$\xi = c_1 \cdot S_{dq95} + c_2 \cdot \frac{1}{S_{al}} \tag{1}$$

where $S_{\mathrm{dq95}} = P_{95}\left[g(x,y)\right]$ denotes the 95th percentiles of the gradient magnitude distribution. The local gradient $g(x,y)$, describing the surface geometry, is defined as [15]

$$g(x,y) = \sqrt{\left(\frac{\partial z}{\partial x}\right)^2 + \left(\frac{\partial z}{\partial y}\right)^2} \tag{2}$$

The parameter S_{al} denotes the autocorrelation length of the surface, representing the characteristic lateral scale of surface features. Its inverse, $1/S_{al}$, reflects the compactness of the topography, i.e., the spatial density of surface structures.

This descriptor ξ therefore combines the upper-tail slope content (S_{dq95}), representing the presence of steep features, and lateral compactness ($1/S_{\mathrm{al}}$), representing the spatial density of surface structures. High values of ξ correspond to surfaces with steep and densely distributed features, which are more prone to optically induced distortions such as multiple reflection, shadowing, and scattering.

To ensure comparability of the contributing terms, S_{dq95} and $1/S_{\mathrm{al}}$ are normalized by appropriate reference values. The coefficients c_1 and c_2 therefore act as dimensionless weighting factors that balance the relative influence of slope content and lateral compactness.

3.2 Physics-based semi-analytical framework

The observed FOV-dependent distortions arise from the combined influence of (i) local surface geometry, (ii) global surface complexity, and (iii) the position-dependent response of the optical system.

The local surface slope angle is defined as

$$\theta(x, y) = \arctan\big(g(x, y)\big), \tag{3}$$

where $g(x, y)$ is the local gradient of the surface.

Optical topography measurements of complex surfaces are affected by a progressively increasing loss and distortion of high-angle information as the measurement position moves away from the centre of the FOV.

To describe this effect, an angular–complexity–position-dependent transfer model is introduced:

$$T = T(\theta, \xi, r) \tag{4}$$

where θ denotes the local surface slope angle, ξ is a non-local descriptor of surface complexity, and $r = (x, y)$ represents the position within the FOV. Here, T represents an effective transfer or fidelity function describing the degree to which surface features are correctly captured under given angular, surface, and positional conditions.

To first order, the transfer function can be expressed as

$$T(\theta, \xi, \mathbf{r}) = T_\theta(\theta, \mathbf{r}) \cdot T_\xi(\xi, \mathbf{r}) \tag{5}$$

where $T_\theta(\theta, \mathbf{r})$ describes the angular transfer behavior, primarily governed by the local slope and the position-dependent angular acceptance of the system, $T_\xi(\xi, \mathbf{r})$ accounts for additional surface-dependent effects such as scattering and inter-feature interactions. This separable formulation represents a first-order approximation, assuming that angular and complexity-driven effects can be treated independently.

This framework highlights that, for complex surfaces, measurement limitations are governed by a coupled angular–structural interaction, rather than by angular acceptance alone.

4. CONCLUSIONS AND OUTLOOK

This work demonstrates that FOV effects in confocal laser scanning microscopy (CLSM) are inherently surface-dependent and cannot be explained by local slope alone. While smooth geometries show negligible FOV influence, complex surfaces with high spatial frequency content exhibit pronounced, position-dependent distortions, as evidenced by the strong variation of height parameters and slope distributions across the FOV.

The results reveal that CLSM measurement behaviour is governed by a coupled interaction between local slope and surface complexity. For complex surfaces, CLSM measurements become increasingly instrument-limited, due to position-dependent loss of high-angle information associated with scanning-induced effects such as pupil shift, pupil clipping, and off-axis aberrations.

To interpret these effects, a semi-analytical framework $T(\theta, \xi, \mathrm{r})$ was introduced, linking local slope, surface complexity, and FOV position. The proposed descriptor $\xi = c_1 S_{\mathrm{dq95}} + c_2/S_{\mathrm{al}}$ provides a unified description of angular limitations and surface-dependent effects, offering a physically grounded interpretation of FOV distortions. This has direct implications for traceability, as conventional calibration approaches based on simple geometries may not be representative for complex surfaces.

Future work will focus on quantifying the transfer function components, integrating the model into uncertainty evaluation, and developing representative calibration strategies for complex surfaces. These developments are essential for achieving traceable and application-relevant optical surface metrology beyond conventional geometry-based approaches.

REFERENCES

[1] de Groot, P., "Principles of interference microscopy for the measurement of surface topography," *Adv. Opt. Photon.* 7(1), 1–65 (2015)

[2] Kim, C.-S., and Yoo, H., "Three-dimensional confocal reflectance microscopy for surface metrology," *Meas. Sci. Technol.* 32, 102002 (2021)

[3] Reitbauer, J., Harrer, F., Eckhart, R., and Bauer, W., "Focus variation technology as a tool for tissue surface characterization," *Cellulose* 28, 6813–6827 (2021)

[4] Leach, R., *Optical Measurement of Surface Topography*, Springer, Berlin (2011)

[5] Pawlus, P., Reizer, R., and Wieczorowski, M., "Comparison of surface topography measurements obtained by optical methods," *Metrol. Meas. Syst.* **25**(3), 589–602 (2018)

[6] Tosello, G., et al., "An international comparison of surface texture parameters quantification on polymer artefacts using optical instruments," *CIRP Annals*, 65 (1), 529-532 (2016)

[7] Leach, R., Giusca, C., Haitjema, H., Evans, C., and Jiang, X., "Calibration and verification of areal surface texture measuring instruments," *CIRP Ann. Manuf. Technol.* 64(2), 797–813 (2015)

[8] Gao, S., Felgner, A., Brand, U. and Koops, R., "Influence of the inhomogeneity of the field of view on the measurement of surface texture in optical surface topography measuring instruments," *Proc. euspen Int. Conf.*, 262-265 (2025)

[9] de Groot, P. "Coherence Scanning Interferometry" In: Leach, R. (eds) *Optical Measurement of Surface Topography*. Springer, Berlin, Heidelberg (2011)

[10] Jiang, X., Scott, P. J., Whitehouse, D. J., and Blunt, L., "Paradigm shifts in surface metrology. Part II. The current shift," *Proc. R. Soc. A* 463(2085), 2071-2099 (2007)

[11] ISO 25178-700:2022, Geometrical Product Specifications (GPS)—Surface texture: Areal—Part 700: Calibration, adjustment and verification of areal topography measuring instruments, *ISO*, Geneva (2022)

[12] https://www.simetrics.de/en/downloads/RnS.pdf

[13] Pawley, J. B. (Ed.), *Handbook of Biological Confocal Microscopy*, 3rd ed., Springer, New York (2006)

[14] Wilson, T., and Sheppard, C. J. R., "*Theory and Practice of Scanning Optical Microscopy*", Academic Press, London (1984)

[15] ISO 25178-2:2021, Geometrical Product Specifications (GPS)—Surface texture: Areal—Part 2: Terms, definitions and surface texture parameters, *ISO*, Geneva (2021)